APPLIED SPECTROSCOPY REVIEWS, 19(2), 259-323 (1983)

Vibrational Spectra of Layer Crystals

PRADIP N. GHOSH
Department of Physics
University of Calcutta
Calcutta 700009, India

I. INTRODUCTION 260

II. LAYER STRUCTURES. 261
A. Metal Halides 266
B. Metal Hydroxides 268
C. Metal Dichalcogenides 268
D. Binary Compounds 271
E. Orpiment 274
F. Charge Density Wave States. 274

III. SYMMETRY AND VIBRATIONS OF LAYER CRYSTALS . 275
A. Layer and Crystal Symmetry 275
B. Group Theoretical Analysis 278

IV. EXPERIMENTAL OBSERVATIONS 291
A. Metal Halides 291
B. Metal Hydroxides 298
C. Metal Dichalcogenides 299
D. Binary Compounds 304
E. Orpiment Structures 307
F. Ternary Compounds 310

V. LAYER DYNAMICS CALCULATIONS 311

VI. SUMMARY 315

References 317

0570-4928/83/1902-0259$3.50/0

I. INTRODUCTION

Layer crystals have received considerable attention of spectroscopists because of the wide range of electrical and optical properties they possess. The group of layered chalcogenide crystals contains insulators, semiconductors, metals, and superconductors at moderately high temperature. The layered halide crystals act as reliable hosts for Jahn-Teller, ESR, and other optical experiments. The layerlike nature of such crystals leads to experimentally distinguishable lattice optical properties. The existence of layer and crystal symmetries is clearly manifested in the vibrational spectra of these crystals which have been determined in recent years by means of infrared and Raman investigations of the zone center modes. The large anisotropy of electrical properties leads to LO-TO splitting, while the small interlayer interaction gives rise to Davydov-type splitting besides low frequency interlayer modes. Thus investigations of such crystals have been a considerable addition to our knowledge of the vibration spectra of crystals, in general. In fact, a few of these studies provide very transparent examples of the subject.

The research on vibrational spectra of layered $Mg(OH)_2$ crystals started as early as 1905 [1]. This was followed by a number of other investigations [2-6]. The rapid developments in infrared instrumentation and Raman scattering techniques, particularly after the availability of different kinds of lasers, have given a new spurt to activities in spectroscopic research. With the developments of these techniques it has become possible to record the low frequency vibrational spectra of crystals with very high resolution for which an unambiguous assignment is possible. Modern research on the vibrational spectra of layer crystals was initiated by the two pioneering works of Zallen, Slade, and Ward [7] and Wieting and Verble [8] which were published in the same issue of Physical Review B. The first half of the 1970s has observed a large number of reports on the first-order vibrational spectra of the simplest polytypes of layer compounds. Most of these studies have been reviewed recently [9]. However, the latter part of the 1970s has been marked by a series of new techniques like the resonance Raman process and also by studies on the new low-temperature phase of layer crystals known as charge density wave states. The periodic distortion of structures associated with the formation of charge density waves [10] is clearly manifested in their vibrational spectra. Reference 9 contains a review of literature until 1976, hence many of these recent investigations were not included. In the present article we emphasize the recent developments and provide a complete account of the field. We have taken care to avoid repetition of the results already reviewed [9].

Section II provides a brief description of different types of layer structures. We attempt to present a comprehensive list of all the known members in the family tree of layer crystals. In Section III we discuss the symmetry of layer crystals where proper emphasis has been given to the diperiodic group [7, 11] of layer symmetry and the triperiodic group of crystal symmetry. Wieting and Verble [9] have presented the correlation method [12, 13] of analysis of symmetry modes of different types of symmetries. Since most of the experimental studies reported in the literature carry out factor group analysis [14] of normal modes, we present the method and analysis based on this method for all the different types of symmetry. We also emphasize the interlayer interaction Davydov splitting as distinct from factor group splitting in molecular crystals [15]. In Section IV we have collected recent experimental observations, particularly those on higher polytypes, charge density wave states, resonance Raman scattering and second-order processes, etc. The last section contains a brief review of different types of theoretical model calculations attempted so far for an interpretation of the observed data.

II. LAYER STRUCTURES

A layer crystal consists of stacked individual layers. Each layer consists of a few sublayers of atoms which are held together by forces that are presumably intermediate between ionic and covalent. The layers are held together by weak van der Waals forces to form a crystal. Each layer, consisting of the atomic sheets or sublayers which constitute it, has a slablike shape. Within each atomic sheet the atoms are infinitely periodic in two dimensions. Thus one individual layer is a three-dimensional entity, but it has periodicity only in the two dimensions parallel to the layers, lacking periodicity in the third. A layer can be regarded as a gigantic molecule in which all the atoms are bound together by relatively strong intramolecular (or intralayer) forces. The molecules (or layers) are then held together by considerably weaker intermolecular (or interlayer) forces to form a crystal.

Each layer may be regarded as a network solid in the two directions parallel to the layers, while the addition of a third direction perpendicular to the layers makes them molecular solids. In graphite, p-orbitals normal to the plane of atoms overlap to form π-molecular orbitals covering the entire layer. They form partly filled conduction bands; this makes them semimetals parallel to the layers while the weak interlayer interaction perpendicular to the layers makes them insulators in this direction. It may be remarked here that graphite is an example of layer

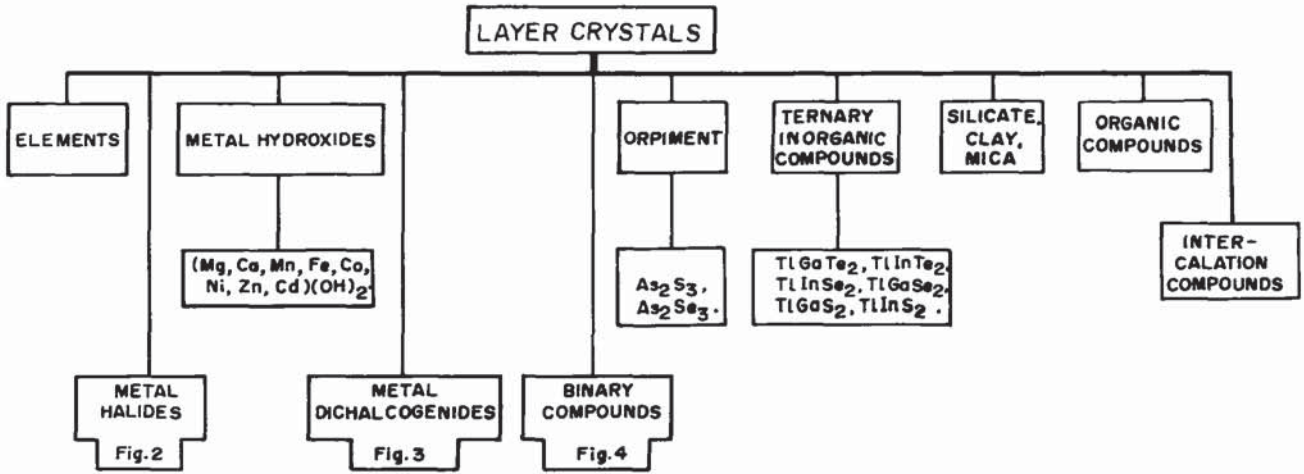

FIG. 1. Classification of layer crystals.

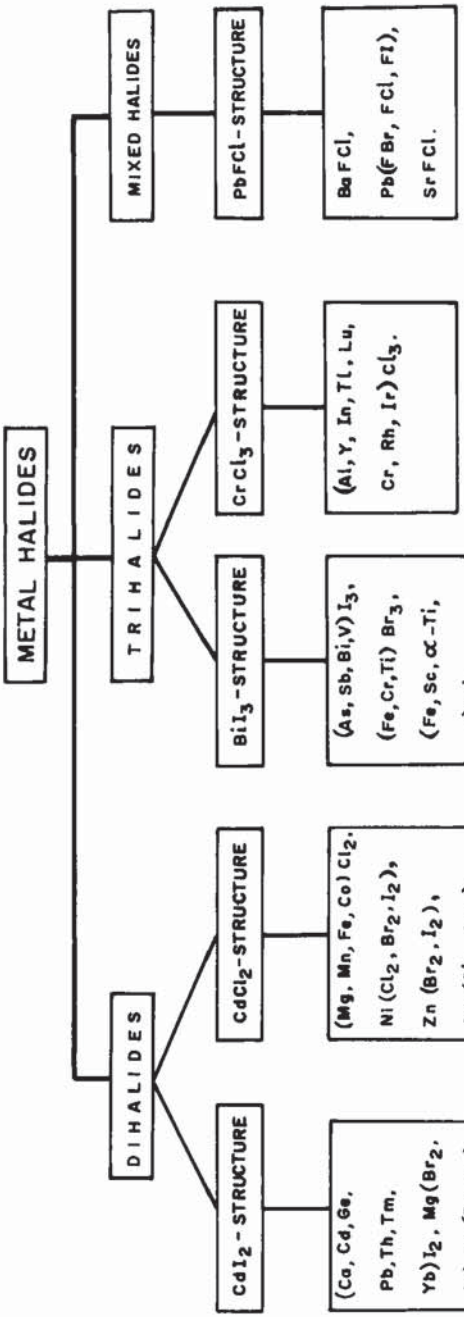

FIG. 2. Layered metal halides.

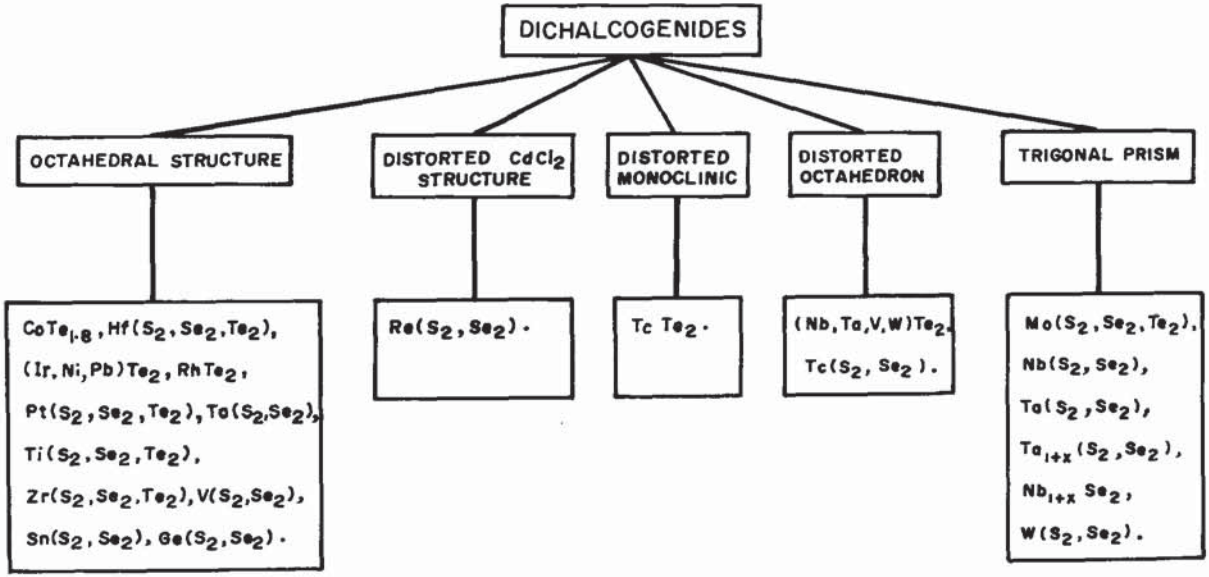

FIG. 3. Layered metal dichalcogenides.

crystals in which each layer is constituted by a single sublayer or atomic sheet. The layered form of graphite and its intercalation compounds have been studied in great detail. The structures of graphite and the isoelectronic crystal BN have been described by Hooley [16]. We will not go into the details of these structures because they are not very important from the point of view of vibrational spectroscopy.

The difference in stacking sequence of the individual layers within a crystal leads to different polytypes [17]. The layers may be stacked exactly parallel to each other so that equivalent atoms belonging to all the layers fall on a straight line perpendicular to the layers. In this case the layer unit cell (the smallest three-dimensional unit that repeats in two dimensions) is identical to the crystal unit cell (the smallest three-dimensional unit that repeats in three dimensions). In other cases the layer stacking may be such that the translation of one single layer to the next layer above or below it in the direction perpendicular to the layer does not reproduce the crystal, but the translation of a set of more than one such layers is repetitive in the third direction. Hence a crystal unit cell having three-dimensional periodicity contains more than one layer unit cells. 2H-PBI_2 has a one-layer crystal unit cell whereas 4H-PbI_2 has a two-layer crystal unit cell, although individual layers in these different crystals are sandwiched identically.

The large family of layer crystals may be classified into a few groups (Fig. 1), some of which may be further divided into different subgroups according to their structural composition. Our discussion in

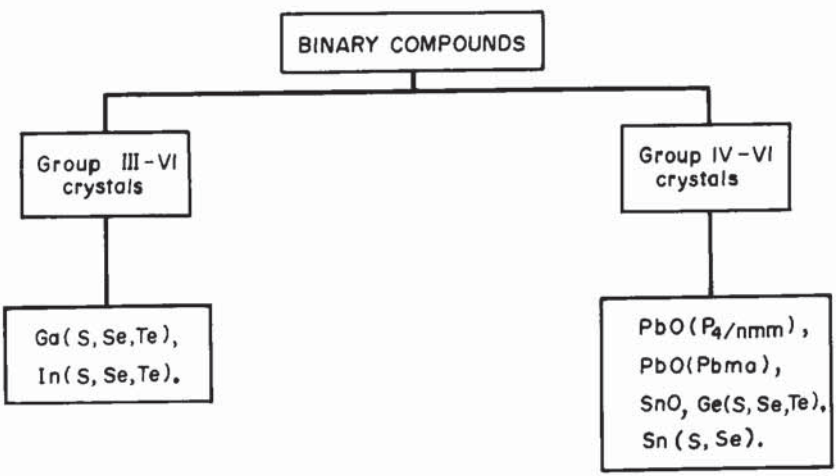

FIG. 4. Layered binary compounds.

this article will be mainly confined to those crystals which have received more attention from vibrational spectroscopists and which offer detailed and very rich information about the bonding nature in these crystals. Figures 1–4 provide a more or less exhaustive list of layered compounds belonging to the metal chloride, metal hydroxide, transition metal dichalcogenides, and binary compound branches in the family tree of layer crystals. Obviously, only a few of them have been experimentally accessible to vibrational spectroscopists. The exact space group to which a structure belongs depends on the polytype. The lowest possible polytype is shown in the figure for those crystals which have a number of polytypes.

In the following we present a discussion of important layer structures. A few more crystals, like the ternary compounds, have been spectroscopically studied recently. They are discussed separately in the Section IV.

A. Metal Halides

The more abundant metal halides are the compounds having one formula unit AX_2 in a layer unit cell; the other types have AX_3 or AXY structures (A = metal; X, Y = halogen). The metal dihalides are found to crystallize mainly in two different space groups [18]. The CdI_2-type crystals [18] have a D_{3d}^3 space group with one layer unit cell in a crystal unit cell. The metal ions are octahedrally surrounded in a cage and occupy half of the octahedral interstices (Fig. 5). All the halogen atoms are close packed and alternately placed above and below the sheet of metal atoms. In $CdCl_2$-type crystals [18] the atomic distribution within each layer is identical to that of CdI_2-type crystals, but the stacking sequence is different. They belong to the space group D_{3d}^5 with three layers forming a repetitive unit in the third direction (Fig. 6). Although a crystal unit cell encompasses three layers, each crystal unit cell contains only the same number of atoms as in a single layer. The CdI_2 has a hexagonal close packing ABABAB (Fig. 5) while the $CdCl_2$ has a cubic close packing ABCABC (Fig. 6). A few of the $CdCl_2$ crystals (e.g., $FeCl_2$) are compressible and undergo structural phase transition at high pressure to the hexagonal CdI_2 structure [19, 20].

The choice of a metal dihalide crystal in adopting either the CdI_2 or $CdCl_2$ structure depends on the polarizing effects. Those compounds having a marked polarization effect usually adopt a CdI_2 structure, whereas the others with moderate polarization crystallize with a $CdCl_2$ structure. Thus, except for a few cases, the CdI_2-type contains mostly bromides and iodides, while the $CdCl_2$ type contains mainly the chlorides. The less important metal trihalides adopt $CrCl_3$ or BiI_3-type structures [18]. The mixed halides are typified by the PbFCl structure.

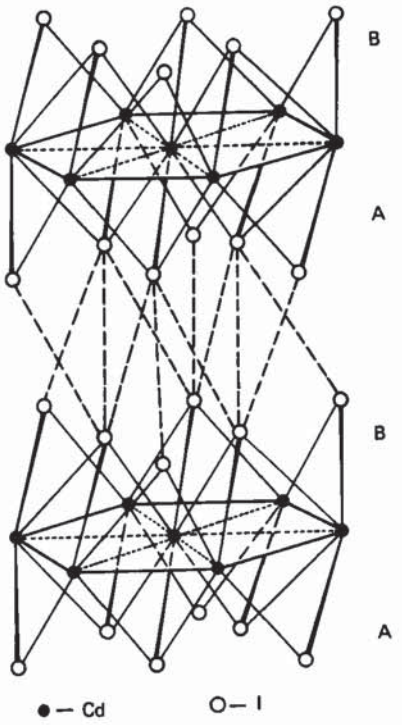

FIG. 5. Cadmium iodide structure.

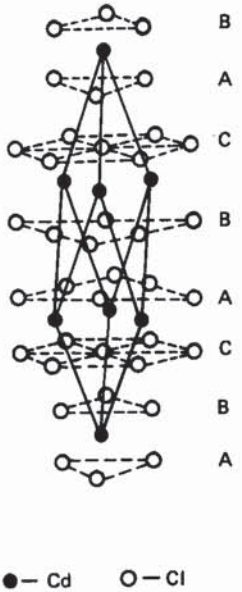

FIG. 6. Cadmium chloride structure.

Although most of these trihalides and mixed halides have been prepared in laboratories, very few spectroscopic experiments have been reported on such crystals. The thermochemical properties and structure of such crystals have been reviewed in great detail by Schoonman and Lieth [18].

B. Metal Hydroxides

Metal hydroxides normally crystallize in a CdI_2 structure where the OH ions occupy the position of the iodine atom and each of them forms three bonds with the bivalent metal atoms, leading to a hexagonal close-packed structure. Such crystals have a single layer unit cell per crystal unit. The proton arrangements and bond distances preclude the possible existence of hydrogen bonding between the layers. Besides the above-mentioned structure, a few bivalent metal hydroxides also adopt several polymorphic configurations [21]. A peculiar feature of the hydroxide layer crystals is that the negative ions are molecular in nature so that each layer contains two molecular OH^- units which comprise a formula unit. Hence these crystals, in addition to being layered, also possess the properties of a true molecular crystal.

C. Metal Dichalcogenides

This group of crystals comprises mainly transition metal dichalcogenides. They form a very distinguished class of layer crystals because of their wide ranging electrical, magnetic, and chemical properties. The easy cleavage property and the possibility of putting in foreign atoms or ions between the layers have received the special attention of scientists in different fields.

Nearly two-thirds of the large number of metal dichalcogenides identified so far crystallize in layered structures. The compounds with Groups VII and VIII metals are nonlayered. Those materials which adopt layer structure can be classified in the following way: octahedral (CdI_2 type), distorted $CdCl_2$ type, distorted octahedran, distorted monoclinic, and trigonal prismatic. Figure 3 contains a list of crystals belonging to these different categories. The crystals having an octahedral CdI_2 structure [22] have a layer unit cell identical to that of CdI_2 (or $CdCl_2$, which has a layer unit cell identical to that of CdI_2). However, the layer stacking is mostly hexagonal close packing which corresponds to CdI_2 and not to $CdCl_2$. In a few cases the structure is slightly distorted in such a way that the metal atom is displaced from the center of the coordination unit. In order to balance the resultant strain due to such displacements, chalocogen sheets bend to give a distorted structure.

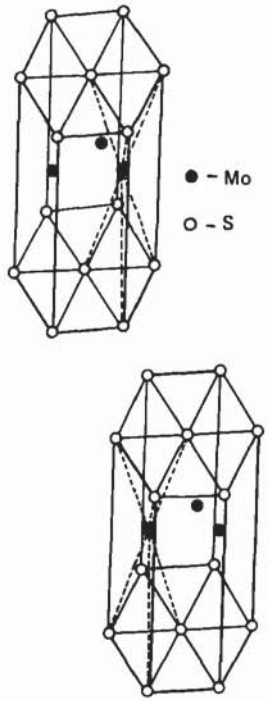

FIG. 7. Molybdenum sulfide structure.

The more interesting compounds in this group are those of the trigonal prismatic type [22]. The most important in this group is MoS_2; that is why the crystals belonging to this group are known as MoS_2 types (Fig. 7). The metal atom is at the center of a prism and coordinated to the six chalcogen atoms which sit at the six corners of the prism. A layer is formed by placing alternately occupied and unoccupied (by metals) prisms side by side. When six such prisms join together to form a hexagonal prism, there are three metals within the hexagonal prism. However, all the corners in both upper and lower faces are occupied by chalcogen atoms. In the octahedral CdI_2 type, one metal is at the center of a hexagonal prism and the nonmetal atoms occupy alternately upper and lower corners of the prism (Fig. 8a). The MoS_2 crystals (Fig. 8b) contain a nonmetal sitting on top of another nonmetal along the Z-axis (perpendicular to the layers), while the CdI_2 crystals do not contain two nonmetal atoms of one layer unit cell along the Z axis (Fig. 8a). This causes a difference in symmetry property of the

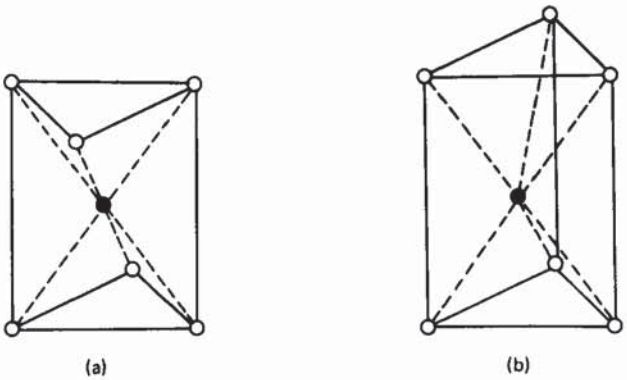

FIG. 8. Octahedral (a) and trigonal (b) prismatic coordination.

normal modes of vibration. However, both of these structures have a metal plane sandwiched between two nonmetal planes.

The stacking of these layers is found to result in a number of polytypes which may be defined as a special kind of one-dimensional polymorphism [17]. There can be 1, 2, 3, 4, or 6 layer units forming a repetitive unit in the c-direction. In a polytype containing n layer units per crystal unit cell, the layer units are rotated with respect to one another such that the first and the (n + 1)-th layer units are identically placed so that the equivalent atoms fall on a straight line drawn parallel to the Z-axis. For a trigonal prismatic type (MoS_2), the one layer crystal unit cell is not known. Thus the lowest member of the polytype series is 2H (2 stands for two layers per crystal unit and H for hexagonal

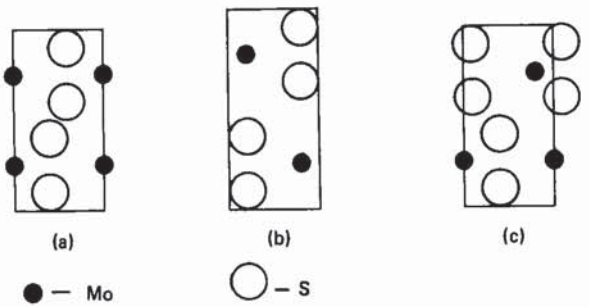

FIG. 9. Three different polytypes of 2H-MoS_2: (a) 2Ha, (b) 2Hb, and (c) 2H.

unit). Again the stacking of the two layers in a repetitive unit can be in three different ways, giving three possible configurations of the 2H polytype (Fig. 9). Similarly, higher polytypes can be formed and found in a number of possible stacking sequences [22]. In a similar way, octahedral layer units are found to result in the polytypes 1T, 2H, 3R, and 6R. TaS_2 is known to exist in all these polytype configurations. There are possibilities of further polytypes having alternately prismatic and octahedral surroundings of metal atoms. The chalcogenides of Ta and Nb are known to exhibit this kind of polytypism.

TaS_2 and $TaSe_2$ can undergo phase transition from normal to a charge density wave (CDW) state [23]. These are discussed separately in Section II-F.

D. Binary Compounds

The binary compounds which crystallize with layer structures can be broadly classified into two types, III-VI and IV-VI, where the nonmetal atom of both groups belongs to Group VI (e.g., S, Se, Te). The metal atom of III-VI compounds belong to Group III (e.g., Ga, In, Tm) while those of IV-VI compounds belong to Group IV (e.g., Sn, Ge).

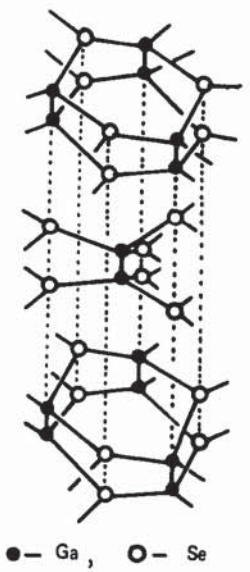

FIG. 10. Crystal structure of ϵ-GaSe.

Each layer is formed by two molecular (or formula) units: two metal (X) sheets are sandwiched between two nonmetal (Y) sheets giving ...Y–X–X–Y... type slabs. The nonmetal atoms are chalcogens while the metal atoms belong to Groups III and IV, and these crystals possess unique physical properties like the dichalcogenides. In fact, the III-VI compounds like GaSe, GaS, and InSe have, perhaps, received the maximum attention of spectroscopists, and these studies have resulted in the largest amount of information on layer structures.

The III-VI layered compounds [24] crystallize in a trigonal prismatic configuration like MoS_2. Instead of one metal at the center of the prism, there are two metal atoms along the central axis (c) of the prism, and each of them is equally placed from the center. Each metal atom is coordinated with three chalcogen atoms at the corners of the prism and the other metal atom (Figs. 10-12). Similar to the dichalcogenides, these crystals also form a number of polytypes. GaSe is found to crystallize with two or three layer units per crystal unit cell known respectively as ϵ- and γ-types. Such structures result from the relative

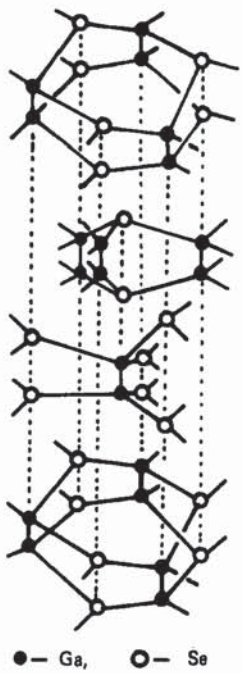

FIG. 11. Crystal structure of γ-GaSe.

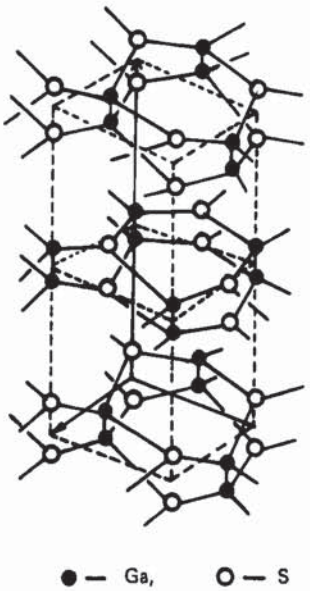

FIG. 12. Crystal structure of β-GaS.

translation of one slab with respect to another (Figs. 10 and 11). GaS is known to have only one polytype with two layers in a crystal repetitive unit known as the β-type. In this case, one layer unit is rotated with respect to the other and translated in the hexagonal direction (Fig. 12). It may be noted that in the earlier days ϵ-GaSe was often referred to as β-GaSe. This was later corrected [24].

InSe [25] crystallizes mostly in a γ-type rhombohedral unit as in γ-GaSe (Fig. 11). However, the crystals grown by Bridgman's method show that hexagonal ϵ-polytypes also form, although the γ-types are more abundant. Recently, Kuroda et al. [26] showed that at high pressure InSe undergoes a layer-to-nonlayer phase transition, and the nonlayer phase is monoclinic.

InS crystallizes with space group D_{2h}^{12}, having two layers per unit cell [27, 28]. Each layer is formed by four atomic planes in the order $-S-In-In-S-$ and the layer symmetry corresponds to C_{2h}^{1} (DG 14). An important difference between InSe and InS is that in InSe all the nearest neighbors of an In atom are in one layer, whereas in case of InS two S atoms and one In atom are in the same layer while the third S atom is in a neighboring layer. This produces a remarkable difference in the binding forces and the interlayer force in InS is not very weak

compared to intralayer ones, which is a characteristic property of layer crystals. Some authors prefer not to include InS in the list of layer crystals.

Among the IV-VI layered compounds [29], SnS and SnSe are known and have been studied spectroscopically in detail. GeS, GeSe, and GeTe have also been studied recently.

E. Orpiment

As_2S_3 and As_2Se_3 are found to crystallize with orpiment structure. Each layer contains two formula units, i.e., 10 atoms. Each As atom is coordinated with three nonmetal atoms while each nonmetal atom is coordinated to two As atoms. The crystal has low symmetry with a monoclinic arrangement [30]. There are two layers in a crystal unit cell. Thus the crystal space group is C_{2h}^5. The structures are described in Ref. 7.

F. Charge Density Wave States

The charge density waves (CDW) may be described as periodic variations of the conduction electron density which will produce a periodic lattice distortion resulting in a superlattice structure [10]. As the temperature is lowered below a critical temperature T_c, the phase transition normal→CDW occurs. The formation of CDW state at T_0 was evident from electron diffraction studies of Wilson, Disalvo, and Mahajan [23] who observed weak superlattice Bragg spots in $TaSe_2$ (2H polytype). Just below the onset temperature T_0, the periodicity of the CDW distortion is not an integral multiple of the lattice spacing. Hence, such a phase may be described as incommensurate CDW (ICDW). Neutron scattering studies of Moncton, Axe, and Disalvo [31] on $TaSe_2$ showed that at $T_0 = 122.3$ K a superlattice structure develops which is not commensurate with the high temperature reciprocal lattice of the normal phase. The wave vector in the new phase is given as $(1 - \delta)a^*/3$, where $a^* = 4\pi/\sqrt{3}a$, $\delta = 0.02$, and a is the lattice spacing for the hexagonal polytype, and was found to be temperature dependent. At 90 K, $\delta \rightarrow 0$ and the superlattice is exactly commensurate (CCDW) with the high temperature lattice with $a' = 3a$ and $c' = c$. A similar experiment [31], carried out on 2H-$NbSe_2$, also showed a phase transition normal→ICDW at $T_0 = 33.5$ K; surprisingly, the deviation from commensurability δ was found to be the same as in 2H-$TaSe_2$. However, no lock-in transition ICDW→CCDW was found for this crystal above 5 K. A similar normal→CDW phase transition has been found in 2H-TaS_2 at 78 K by Holy et al. [32].

As discussed in Section II-C, TaS_2 and $TaSe_2$ can also exist in the 1T-polytype. 1T-TaS_2 and 1T-$TaSe_2$ similarly exhibit phase transition to CDW states [33]. Below 180 K in 1T-TaS_2 and 473 K in $TaSe_2$, the CDW state is commensurate with the CdI_2-type host lattice. The supercell is triclinic and has the dimensions $\sqrt{13}a_0 \times \sqrt{13}a_0$ for the basal plane and a thickness of one layer. The unit cell of this commensurate phase has 39 atoms. Between 220 and 350 K the CDW distortion in 1T-TaS_2 is very close to that of the low-temperature commensurate phase, which has been referred to as quasi-commensurate. Above 370 K in 1T-TaS_2 and 473 K in 1T-$TaSe_2$ the CDW distortion is not periodic with the normal phase and what results is an incommensurate CDW state.

III. SYMMETRY AND VIBRATIONS OF LAYER CRYSTALS

The layer crystals are composed of infinitely extended two-dimensional molecular units. Hence the group theoretical analysis of the observed spectra should include the diperiodic layer symmetry as well as the triperiodic crystal symmetry. Any difference in the symmetry nature of the layer and the crystal will lead to a difference in the phonon-photon selection rule. Hence a clear understanding of the layer and crystal symmetry is necessary for interpretation of the observed vibrational spectra.

A. Layer and Crystal Symmetry

A layer may be defined as a two-dimensional slab. The slab is infinitely extended in two dimensions parallel to its surface, but it also has a third dimension perpendicular to the surface because of the finite thickness of the slab. Each slab consists of a few sheets of atoms. Such a layer belongs neither to one of the 230 three-dimensional space groups having three dimensional periodicity in a three-dimensional space nor to one of the 17 two-dimensional space groups having two-dimensional periodicity in a two-dimensional space. They have a two-dimensional periodicity in a three-dimensional space and thus belong to one of the 80 diperiodic space groups listed by Wood [11]. A detailed discussion on diperiodic groups in layer crystals is given by Zallen, Slade, and Ward [7].

The space group of a layer consists of the symmetry operations $\{R^F | \chi(\ell)\}$, where R^F consists of the factor group operations, i.e., they contain the point group operations together with nonprimitive translations $\chi(R)$ in a three-dimensional space, e.g., the screw-axis and glide plane operations. Hence R^F may be written as $\{R | \chi(R)\}$;

$\underset{\sim}{\chi}(\ell)$ denotes a two-dimensional vector having components parallel to the plane of layers and consists of primitive translations. It may be noted that $\underset{\sim}{\mu}(R)$ does not exist in the 17 two-dimensional space groups. They do exist in the 230 three-dimensional space groups; however, in the case of a layer, $\underset{\sim}{\chi}(\ell)$ is only two-dimensional. The factor group consisting of operations R^F is isomorphous to one of the 32 point groups. If the nonprimitive translations $\underset{\sim}{\mu}(R)$ are zero, the factor group becomes identical to one of the point groups. This case would be analogous to the symmorphic space group of the 230 space groups. In the case of layer symmetry the factor groups contain the screw axis or glide plane operations. In fact, it is these operations which make them distinct from a pure two-dimensional system. Thus the space groups of layers are usually nonsymmorphic. As pointed out by Wood [11], there are 80 combinations of symmetry operations $\{R^F | \underset{\sim}{\chi}(\ell)\}$.

A real crystal containing the layers stacked one above another in some particular fashion also has a periodicity in the third direction perpendicular to the layers. Hence the space group consists of the symmetry operations $\{R^F | \underset{\sim}{\rho}(\ell)\}$, where $\underset{\sim}{\rho}(\ell)$ consists of primitive translations in three dimensions. Thus the crystal symmetry corresponds to one of the 230 space groups and all the usual definitions of space group are applicable to layer crystals. The factor group operations R^F are defined similarly but they apply to the crystal as a whole, not to the layer. If the primitive unit cell contains only one layer, the factor group of the crystal is identical to that of the layer. This is the case in 2H-CdI_2 where both the crystal and the layer factor groups are isomorphous to the D_{3d} point group. However, if the crystal primitive unit cell encompasses more than one layer, the layer and the crystal factor groups are not identical. For example, 2H-MoS_2 and β-GaS have layer factor groups isomorphous to the D_{3h} point group, whereas the crystal factor group is isomorphous to the D_{6h} point group. In such a case the crystal primitive unit cell contains atoms of two successive layer unit cells, hence its size is exactly double that of a layer unit cell (Figs. 7 and 12). It is shown later that the presence of a center of inversion in the crystal factor group (e.g., D_{6h}) leads to the characteristic gerade and ungerade symmetry species having specific selection rules which are absent in the layer symmetry.

In the above example the layer factor group is a subgroup of the crystal factor group. However, this is not always the case. In fact, the completely reverse case is found in γ-GaSe where the crystal factor group C_{3v} is a subgroup of the layer factor group D_{3h}. This means that the layer factor group has more symmetry elements. This leads to a

TABLE 1

Layer and Crystal Symmetries of Different Types of Crystals

Type	Number of formula units in a layer unit cell	Number of layers in a crystal unit cell	Layer symmetry		Crystal symmetry	
			Factor group	Diperiodic group	Factor group	Space group
CdI_2	1	1	D_{3d}	DG 72	D_{3d}	D_{3d}^3
$CdCl_2$	1	3[a]	D_{3d}	DG 72	D_{3d}	D_{3d}^5
4H-CdI_2	1	2	D_{3d}	DG 72	C_{6v}	C_{6v}^4
2H-MoS_2	1	2	D_{3h}	DG 78	D_{6h}	D_{6h}^4
3R-MoS_2	1	3[a]	D_{3h}	DG 78	C_{3v}	C_{3v}^5
3T-MoS_2	1	3	D_{3h}	DG 78	C_{3v}	C_{3v}^1
ϵ-GaSe	2	2	D_{3h}	DG 78	D_{3h}	D_{3h}^1
γ-GaSe	2	3[a]	D_{3h}	DG 78	C_{3v}	C_{3v}^5
β-GaS	2	2	D_{3h}	DG 78	D_{6h}	D_{6h}^4
SnS	2	2	C_{2v}	DG 32	D_{2h}	D_{2h}^{16}
As_2S_3	2	2	C_{2v}	DG 32	C_{2h}	C_{2h}^5

[a]One primitive unit cell spans three layers, but contains the same number of atoms as a single layer (see text).

paradoxical situation because, according to our definition, the crystal primitive unit cell contains one or more than one layer unit cells. In this case, since the crystal factor group is not identical to the layer factor group, the crystal primitive unit cell has to contain atoms from more than one layer unit cells. It does indeed contain atoms from three successive layer unit cells, but it spans only three layers and does not embrace three complete layer unit cells, as in the case of 2H-MoS_2 embracing two layer unit cells. This resolves the paradox: the crystal primitive unit cell contains two molecules as does a layer unit cell. As we shall see subsequently, we would not expect a reverse correlation field splitting from the crystal to the layer factor group. The layer crystal compatibility relation for 2H-MoS_2 will show correlation field splitting. A similar situation is true for $CdCl_2$ where the crystal primitive unit cell spans three layers but contains only one molecule. In this case the crystal factor group and the layer factor groups are both isomorphous to the D_{3d} point group. Yet the primitive unit cell of the crystal is not identical to that of the layer, hence the factor group operations act on different basis vectors. This makes the crystal structure distinct from 2H-CdI_2 in which a layer unit cell is identical to that of $CdCl_2$. They belong to the same diperiodic group, however.

The orpiment (As_2S_3) structure has a relatively lower symmetry compared to other common crystals. The layer symmetry corresponds to the diperiodic group DG 32, and the layer factor group C_{2v} is not a subgroup of the crystal factor group C_{2h}. In this case the layer symmetry if orthorhombic, whereas the crystal symmetry is monoclinic. It may be noted the actual layer factor group is C_s; however, if the atoms are displaced by an amount smaller than the experimental error of X-ray data, we get the orthorhombic structure [7].

The layer and crystal symmetry of a few common layer crystals are collected in Table 1. This table contains data for SnS-type crystals which have been studied recently and are not contained in the earlier layer structure studies [29]. The layer symmetry is C_{2v} with a molecular S−Sn−Sn−S unit, and the crystal contains two layers with D_{2h} symmetry.

B. Group Theoretical Analysis

The existence of high symmetry in layer crystals shows that group theory would play an important role in analyzing the vibrational spectra of layer crystals. The methods of group theoretical analysis for the vibrational spectra of solids have been described in detail in the literature. The most widely used method is that of Bhagavantam and Venkatarayudu [14] who first proposed factor group analysis of the vibrational modes. The method uses the standard prescriptions of group

theoretical analysis for finding the normal modes of a polyatomic molecule belonging to different symmetry species. In a crystal the factor group operations are used for constructing the reducible representation in a 3n dimensional basis, where n is the number of atoms in a primitive unit cell of the layer or crystal. Besides the work of Bhagavantam and Venkatarayudu [14], the factor group method has been described in detail by Mitra [6], Ross [34], and many others.

The other important group theoretical method is based upon the correlation between the site group of individual atoms and the factor group of the crystal. The method was proposed by Hornig [12] and Winston and Halford [13].

1. Translational Symmetry

In a crystal containing n atoms in a primitive unit cell and N^3 such primitive unit cells form the macroscopic crystal, there are $3nN^3$ degrees of freedom. Hence one has to solve a $3nN^3$-dimensional problem. This is an enormously large number. However, to the great relief of spectroscopists, atomic arrangements within a crystal are symmetric which can reduce the problem to a considerably smaller dimension. The first symmetry one encounters in such analysis and which plays the most significant role is the translational symmetry. These are the set of primitive translations $\underset{\sim}{\rho}$ of the crystal space group $\{R^F|\underset{\sim}{\rho}\}$. In case of the diperiodic group, these are the two-dimensional primitive translations $\underset{\sim}{X}$. (In a layer having diperiodic group symmetry, the total number of degrees of freedom is $3nN^2$.) Hence the first step in group theoretical analysis is to form a set of translationally invariant symmetry coordinates

$$t_i(\underset{\sim}{q}) = N^{-3/2} \sum_{\ell} e^{-2\pi i \underset{\sim}{q} \underset{\sim}{R}(\ell)} r_i(\ell) \tag{1}$$

where $\underset{\sim}{q}$ is a three-dimensional vector in the reciprocal space, $\underset{\sim}{R}(\ell)$ represents the position vector of the ℓ-th unit cell, and $r_i(\ell)$ denotes the displacement coordinates of the i-th atom in the ℓ-th unit cell. This step singles out a set of 3n linear combinations of the displacements of atoms belonging to different unit cells. Hence, instead of considering the complete $3nN^3$-dimensional problem, one can consider a 3n-dimensional problem for each of the N^3 allowed values of $\underset{\sim}{q}$. Thus the complete dynamical problem reduces to a set of N^3 blocks, each block corresponding to one value of $\underset{\sim}{q}$. These different $\underset{\sim}{q}$ values correspond to different phase relations of displacements of equivalent atoms in N^3 primitive unit cells. It is convenient that $\underset{\sim}{q} = 0$ corresponds to a motion where the equivalent atoms in all the unit cells move in phase, and the usual

methods of infrared and Raman spectroscopy correspond to $\underset{\sim}{q} \simeq 0$ [35]. Hence all of our subsequent discussions will be based on an analysis of the 3n-dimensional problem at $\underset{\sim}{q} = 0$. For this purpose one can consider any one primitive unit cell and exploit the full symmetry of the unit cell, i.e., the factor group symmetry. Hence translationally symmetric coordinate may be further symmetrized by the use of factor group symmetry. This process will lead to further block diagonalization of the $3n \times 3n$ dimensional secular determinant. This is discussed in the following subsection.

In this case of an isolated layer, the 3-dimensional space group is replaced by a diperiodic group and the set of translationally invariant symmetry coordinates may be constructed similarly as

$$d_i(\underset{\sim}{q}_d) = N^{-1} \sum_{\ell} e^{-2\pi i \underset{\sim}{q}_d \underset{\sim}{R}_d(\ell)} r_i(\ell) \tag{2}$$

$\underset{\sim}{q}_d$ is a two-dimensional vector in the reciprocal lattice of the layer, $\underset{\sim}{R}_d$ is the position vector of the ℓ-th unit cell in the diperiodic layer, and $r_i(\ell)$ is defined similarly as earlier. There are N^2 unit cells in the diperiodic lattice and hence N^2 possible values of $\underset{\sim}{q}_d$.

2. Factor Group Analysis

The methods of factor group analysis are based upon the full symmetry R^F of the primitive unit cell. The factor group operations R^F comprise rotations (including plane of reflection and center of inversion) and nonprimitive translations. Hence a factor group is a space group $\{R^F | 0\}$. The symmetry operations carried out on an atom of the primitive unit cell brings it into coincidence with another similar atom in the same or a neighboring unit cell. Such atoms which are transformed into each other by symmetry operations are known as equivalent atoms. An atom in a neighboring unit cell differs from its counterpart in the original unit cell only by a primitive translation whose character is unity at $\underset{\sim}{q} = 0$. The nonprimitive translations like those associated with screw axis and glide plane operations are special features of crystal symmetry. These are absent in point group operations which consist of three-dimensional rotations.

The crystal symmetry correctly describes the symmetry of active modes and selection rules. Yet the identity of individual layers leads to some interesting results. In the case of a crystal where the primitive unit cell contains more than one layer, the isolation of a single layer is hypothetical, because equivalent atoms in two successive layers do

not move identically in phase even at $\underset{\sim}{q} = 0$. Hence the description for a single layer cannot be extended to the whole crystal. But if the interlayer interaction is weak, the intralayer modes more or less retain their own identity like the intramolecular modes in a molecular crystal. The discussions on factor group analysis presented below apply to both crystal and layer factor groups. Subsequently we shall discuss the effect of interlayer interaction and layer-crystal compatibility relations.

The idea behind the factor group method is that under the operations of the factor group, some atoms of the unit cell are left invariant. In order to determine which atoms remain invariant, all of the factor group operations must be applied to the unit cell. We have to form a reducible representation for each operation of the factor group with the displacement coordinates for all the atoms of the unit cell forming a 3n-dimensional basis vector. The successive steps to be followed may be listed as follows.

a. Apply each operation of the factor group to the primitive unit cell (which may be thought of as a molecule). These operations include screw-axes or glide planes.
b. Determine the number of atoms ω_R left invariant by an operation R.
c. Evaluate the quantity $(\pm 1 + 2 \cos \Phi_R)$ for each rotational operation R. The positive and negative signs correspond to proper (identity and pure rotations) and improper (plane of reflection, rotation-reflections, etc.) rotation, respectively, by an angle ϕ_R.
d. The character of reducible representation is obtained as

$$\chi'(R) = \omega_R(\pm 1 + 2 \cos \Phi_R) \tag{3}$$

From knowledge of the space group, the factor group can be easily found. The character of the irreducible representation is obtained from the character table of the point group with which the factor group is isomorphous. If g is the number of symmetry elements, i.e., the order of the group, and h_j is the number of group operations contained in the j-th class, we can find the number of times a particular irreducible representation $\Gamma^{\gamma}(R)$ will appear in the reducible representation $\Gamma(R)$ as

$$a^{\gamma} = \frac{1}{g} \sum_j h_j \chi^{\gamma}(R) \chi_j'(R) \tag{4}$$

where $\chi_j'(R)$ is the character of reducible representation of the symmetry operations belonging to the j-th class and $\chi^{\gamma}(R)$ is the character of the γ-th symmetry species of the operation R for the irreducible representation. Since $\chi_j'(R)$ is determined from the above prescription

(Eq. 3), the distribution of all the 3n degrees of freedom among the different symmetry species γ of the irreducible representation can be found from Eq. (4).

The 3n degrees of freedom include 3 motions which correspond to the movement of the entire unit cell and will correspond to acoustic modes. In such a case ω_R is equal to unity and the character for reducible representation is $\chi_j'(T) = (\pm 1 + 2 \cos \Phi_R)$ from Eq. (3), and the distribution of the three acoustic modes among the symmetry species γ are found from Eq. (4). The remaining (3n - 3) degrees of freedom define the optical modes of vibration.

In order that a normal mode be first-order infrared active, the first derivative of the dipole moment with respect to the normal coordinate Q_K should be nonzero and the symmetry of the normal mode should include the product of symmetry species of the initial and final states,

$$\left(\frac{\partial \mu}{\partial Q_K}\right) \langle i | Q_K | f \rangle \neq 0$$

The wave functions for the initial and final states may be represented as products of harmonic oscillator wave functions in the normal coordinates Q_ℓ's. These wave functions have even or odd parity depending on the evenness or oddness of the vibrational quantum number. Hence we have the selection rule $\Delta V_K = \pm 1$ for the K-th normal mode since Q_K has odd parity. To determine which symmetry species is active in the infrared, one has to find the symmetry property of the dipole moment components, because for the γ-th symmetry species to be active we should have

$$\langle \Psi_0^{\gamma} | \mu_\alpha | \Psi_1^{\gamma} \rangle \neq 0 \qquad (\alpha = x, y, z)$$

Since μ_α has the symmetry property of the translational vector with components x, y, and z, the γ-th species can be IR active only if it has the symmetry species of one of these components. Since the symmetry property of the translational components x, y, and z are known from the character table for irreducible representations, one can easily find which symmetry species is IR active.

In a similar manner one can find the Raman activity of a particular symmetry species by noting the symmetry of the components of the polarizability tensor α_{k1} (k1 = x, y, z). Thus a knowledge of the symmetry species of the products x^2, y^2, z^2, xy, yz, and zx would provide Raman activity of a symmetry species.

In the following we present the results of factor group analysis for the commonly occurring high symmetry layer crystals having factor group symmetries D_{3d}, D_{3h}, C_{2v}, D_{6h}, etc. The procedure to be followed may be listed as:

1. Determine the factor group symmetry for the layer and the crystal. This is obtained directly from the crystal structure analysis and the corresponding space group. The factor group symmetry of the layer may be different from that of the crystal according to our previous discussion.
2. Find the character table of the reducible representation according to the prescription set at the beginning of this section.
3. Use Eq. (4) and the character table for the irreducible representation to find the number of modes belonging to the γ-th species.
4. Use $\chi_j'(T)$ for the character of reducible representation to find the number of acoustic modes of a species γ. The remaining ones are optical modes.
5. After these acoustic modes are eliminated, one can easily find which symmetry modes are Raman or IR active according to the symmetry behavior of xx, yy, etc. and x, y, z, respectively, from the character table.
6. All the optical modes which are neither IR nor Raman active are known as inactive modes.

It should be clear that the procedure is similar for both layer and crystal factor groups. The results obtained are different, and finally a correlation may be made between the layer and the crystal factor group modes.

D_{3h} Factor Group. Layer factor groups of MoS_2 and GaSe and crystal factor group of ϵ-GaSe are isomorphous with D_{3h}. The characters of reducible representations and the distribution of modes among the different symmetry species may be derived easily from the above prescription. The final results are collected in Table 2. There is no inactive mode.

D_{3d} Factor Group. All the CdI_2-type crystals belong to the factor group D_{3d}. The simplest polytype has a single layer and 9×9 dimensional representation. The results obtained are presented in Table 3. In this case also all the modes are active. Since $CdCl_2$-type crystals also belong to the same factor group, these results are also applicable to this type.

TABLE 2

Reducible Representation and Mode Distribution (Γ) in Layer Crystals with D_{3h} Factor Group Symmetry

Symmetry operation R	Φ_R (degree)	$\chi_j'(T)$	MoS_2[a]		GaSe[a]		ϵ-GaSe	
			ω_R	$\chi_j'(R)$	ω_R	$\chi_j'(R)$	ω_R	$\chi_j'(R)$
I	0	3	3	9	4	12	8	24
$2C_3$	120	0	3	0	4	0	8	0
$3C_2$	180	-1	1	-1	0	0	0	0
σ_h	0	1	1	1	0	0	0	0
$2S_3$	120	-2	1	-2	0	0	0	0
$3\sigma_v$	0	1	3	3	4	4	8	8
Γ_{total}			$A_1' + 2A_2'' + 2E' + E''$		$2A_1' + 2A_2'' + 2E' + 2E''$		$4A_1' + 4A_2'' + 4E' + 4E''$	
$\Gamma_{acoustic}$			$A_2'' + E'$		$A_2'' + E'$		$A_2'' + E'$	
Γ_{IR}			$A_2'' + E'$		$A_2'' + E'$		$3A_2'' + 3E'$	
Γ_{Raman}			$A_1' + E' + E''$		$2A_1' + E' + 2E''$		$4A_1' + 3E' + 4E''$	

[a]Isolated layer.

TABLE 3

Reducible Representation and Mode Distribution (Γ) in Layer Crystals with D_{3d} Factor Group Symmetry ($CdCl_2$ or CdI_2 type)

Symmetry operation R	Φ_R (degree)	$\chi_j'(R)$	ω_R	$\chi_j'(R)$
I	0	3	3	9
$2C_3$	120	0	3	0
$3C_2$	180	-1	1	-1
i	180	-3	1	-3
$2S_6$	60	0	1	0
$3\sigma_d$	0	1	3	3
	Γ_{total}	$A_{1g} + 2A_{2u} + E_g + 2E_u$		
	$\Gamma_{acoustic}$	$A_{2u} + E_u$		
	Γ_{IR}	$A_{2u} + E_u$		
	Γ_{Raman}	$A_{1g} + E_g$		

C_{2h} and C_{2v} Factor Groups. The low-symmetry crystals As_2S_3 and As_2Se_3 containing four molecular formula units per crystal unit cell correspond to the C_{2h} factor group, while a single layer with two molecules per unit cell corresponds to the C_{2v} factor group. The group theoretical results obtained are presented in Table 4.

D_{6h} Factor Group. The 2H polytype of MoS_2 and β-polytype of GaS belong to this group. Both of them contain two layers in a crystal unit cell. The results are shown in Table 5. The modes are daughter modes obtained from the splitting of the single layer parent modes corresponding to the D_{3h} factor group (Table 2).

C_{3v} Factor Group. The γ-polytype of GaSe and InSe belongs to this group and spans over three layers in a unit cell (Table 6). Similarly,

TABLE 4

Reducible Representation and Mode Distribution (Γ) in Layer Crystals with C_{2v} and C_{2h} Factor Group Symmetries (orpiment)

C_{2v}[a]					C_{2h}[b]				
Symmetry operation R	Φ_R (degree)	χ_j' (T)	ω_R	χ_j' (R)	Symmetry operation R	Φ_R (degree)	χ_j' (T)	ω_R	χ_j' (R)
E	0	3	10	30	E	0	3	20	60
$C_2(z)$	180	-1	0	0	C_2	180	-1	0	0
$\sigma_v(xz)$	0	1	2	2	σ_h	0	1	0	0
$\sigma_v(yz)$	0	1	0	0	i	180	-3	0	0
Γ_{total}		$8A_1 + 7A_2 + 8B_1 + 7B_2$					$15A_g + 15A_u + 15B_g + 15B_u$		
$\Gamma_{acoustic}$		$A_1 + B_1 + B_2$					$A_u + 2B_u$		
Γ_{IR}		$7A_1 + 7B_1 + 6B_2$					$14A_u + 13B_u$		
Γ_{Raman}		$7A_1 + 7A_2 + 7B_1 + 6B_2$					$15A_g + 15B_g$		

[a] Single layer.

[b] Crystal.

TABLE 5

Reducible Representation and Mode Distribution (Γ) in Layer Crystals with D_{6h} Factor Group Symmetry

Symmetry operation R	Φ_R (degree)	χ_j' (T)	2H-MoS_2		β-GaS	
			ω_R	χ_j' (R)	ω_R	χ_j' (R)
E	0	3	6	18	8	24
$2C_6$	60	2	0	0	0	0
$2C_3$	120	0	6	0	0	0
C_2''	180	-1	0	0	0	0
$3C_2$	180	-1	2	-2	0	0
$3C_2'$	180	-1	0	0	0	0
σ_h	0	1	2	2	0	0
$3\sigma_v$	0	1	6	6	8	8
$3\sigma_d$	0	1	0	0	0	0
$2S_6$	60	0	0	0	0	0
$2S_3$	120	-2	2	-4	0	0
i	180	-3	0	0	0	0
Γ_{total}			$A_{1g} + 2A_{2u} + 2B_{2g} + B_{1u} + E_{1g} + 2E_{1u} + 2E_{2g} + E_{2u}$		$2A_{1g} + 2A_{2u} + 2B_{2g} + 2B_{2u} + 2E_{1g} + 2E_{1u} + 2E_{2g} + 2E_{2u}$	
$\Gamma_{acoustic}$			$A_{2u} + E_{1u}$		$A_{2u} + E_{1u}$	
Γ_{IR}			$A_{2u} + E_{1u}$		$A_{2u} + E_{1u}$	
Γ_{Raman}			$A_{1g} + E_{1g} + 2E_{2g}$		$2A_{1g} + 2E_{1g} + 2E_{2g}$	

TABLE 6

Reducible Representation and Mode Distribution (Γ) in Layer Crystals with C_{3v} Factor Group Symmetry

Symmetry operation R	Φ_R (degree)	$\chi_j'(T)$	γ-GaSe		3R-MoS_2		3T-MoS_2	
			ω_R	$\chi_j'(R)$	ω_R	$\chi_j'(R)$	ω_R	$\chi_j'(R)$
E	0	3	4	12	3	9	9	27
$2C_3$	120	0	0	0	0	0	0	0
$3\sigma_v$	0	1	4	4	3	3	9	9
Γ_{total}			$4A_1 + 4E$		$3A_1 + 3E$		$9A_1 + 9E$	
$\Gamma_{acoustic}$			$A_1 + E$		$A_1 + E$		$A_1 + E$	
$\Gamma_{IR, Raman}$			$3A_1 + 3E$		$2A_1 + 2E$		$8A_1 + 8E$	

3R-MoS_2 also corresponds to the crystal factor group of C_{3v} and spans over three layers although the primitive unit cell contains only one molecule. The 3T-MoS_2 has the same factor group and contains three layers, i.e., three molecules. Hence it contains thrice the number of modes in 3R-MoS_2 or a single layer.

It should be mentioned that the above set of tables on group theoretical analysis is only illustrative, not exhaustive. The procedure may easily be extended to other symmetries and higher polytypes if the crystal structure data are completely known.

3. Interlayer Modes and Davydov Splitting

The low frequency rigid layer modes and the splitting of intralayer modes are manifestations of weak but nonzero interlayer forces. In a two-layer crystal unit cell there will be a set of 3n doubly degenerate modes in the limit of vanishing interlayer interaction. When the interaction is switched on, the degeneracy is removed and the result is a pair of closely spaced doublets where adjacent layers vibrate in and out of phase. The three acoustic modes also split up into doublets, one of them remains acoustic and corresponds to rigid translation of the crystal unit cell while the other one becomes an optical mode in which the two layers rigidly vibrate against each other (so-called rigid layer mode);

hence they have a low frequency and depend entirely on the interlayer force.

From the factor group analysis presented in Section III-B-2 it is clear that the vibrational modes corresponding to a single layer of MoS_2, GaS, or GaSe split up into doublets in 2H-MoS_2, ϵ-GaSe, and β-GaS, respectively. The results are summarized in Table 7. A single layer has D_{3h} symmetry for all the polytypes. However, the ϵ- and

TABLE 7

Davydov Splitting in Layer Crystals

2-Layer crystal[a] (D_{3h})	Single layer[b] (D_{3h})	2-Layer crystal[c] (D_{6h})
A_2'' (acoustic)	A_2'' (acoustic)	A_{2u} (acoustic)
A_2'' (IR)		B_{2g} (inactive)
A_2'' (IR)	A_2'' (IR)	A_{2u} (IR)
A_2'' (IR)		B_{2g} (inactive)
$2A_1'$ (Raman)	$2A_1'$ (Raman)	$2A_{1g}$ (Raman)
$2A_1'$ (Raman)		$2B_{1u}$ (inactive)
E' (acoustic)	E' (acoustic)	E_{1u} (acoustic)
E' (Raman, IR)		E_{2g} (Raman)
E' (Raman, IR)	E' (Raman, IR)	E_{2g} (Raman)
E' (Raman, IR)		E_{1u} (IR)
2E'' (Raman)	2E'' (Raman)	$2E_{1g}$ (Raman)
2E'' (Raman)		$2E_{2u}$ (inactive)

[a] ϵ-GaSe

[b] GaS, GaSe, etc.

[c] β-GaS.

β-polytypes with 2 layers in a crystal unit cell possess symmetries of D_{3h} and D_{6h}, respectively. A characteristic feature of the D_{6h} factor group is the presence of a center of inversion symmetry. In such a case the layer vibration E, which is both Raman and IR active, will generate two mutually exclusive crystalline offspring. One of them will inherit all the Raman strength and the other all the infrared strength of the parent layer vibration. In the case of the in-phase (gerade) mode, the electric moments of adjacent layers are antiparallel and cancel out while the Raman tensor components add up. For the out-of-phase (ungerade) mode, the electric moments add up while the Raman tensor components cancel out. No such phenomenon is observed in the case of crystals without a center of inversion (e.g., ϵ-GaSe). Furthermore, one of the split-up components of the Raman active single layer mode will be inactive in a crystal with a center of inversion. In such crystals an accurate measurement of Davydov splitting needs recording of the Raman and IR spectra on the same specimen of the crystal. This is important because the splitting is very small. In the case of crystals without centers of symmetry a single Raman or IR measurement could yield the Davydov splitting.

The larger size of the crystal unit cell results in folding back of the dispersion curves in the c direction, and a larger number of optically active ($\underset{\sim}{q} = 0$) modes results. These results are discussed separately in the next section.

The splitting of intralayer modes arising from the presence of a weak interlayer interaction has its counterpart in molecular crystals. In molecular crystals the factor group analysis of the crystal unit cell with more than one molecule or molecular group will give rise to a splitting of the nondegenerate intramolecular vibrations. These are simply the classical frequency differences of a set of coupled oscillators. This splitting is commonly known as Davydov or factor group or correlation field splitting. In the case of layer crystals it should be noted that the layer symmetry itself corresponds to a factor group (diperiodic group) having screw axes and glide planes. A factor group analysis of the layer symmetry will not accommodate the splitting of intralayer modes. For this purpose, one should carry out a factor group analysis of the crystal symmetry. To avoid confusion in terminology, we retain the term "Davydov splitting" for layer crystals, while the term "factor group splitting" will be used for molecular crystals. Thus the splitting of intralayer modes in 2H-MoS_2 and ϵ-GaSe are classified as Davydov splittings, while the splitting of OH stretching frequency in $Mg(OH)_2$ is an example of factor group splitting. In the latter case, a single layer contains one formula unit, hence two molecular ions OH. The internal vibrations of OH have a much higher frequency than the metal-hydroxyl group vibrations. A unit cell contains

one monoatomic (metal) and two diatomic (hydroxyl) molecular groups. Thus the metal-hydroxyl group vibrations may be termed as lattice vibrations. Since the crystal and layer unit cells are identical, there is no Davydov splitting and all the rigid layer modes are acoustic. The factor group splitting of the OH stretching frequency results from the coupling of OH molecular group vibrations and has nothing to do with interlayer interaction.

IV. EXPERIMENTAL OBSERVATIONS

Experimental studies on the vibrational spectra of layer crystals have been confined mostly to the high symmetry types which may be broadly divided into two classes. The first class consists of binary compounds having the formula units AB. The second class comprises compounds of the type AB_2 among which the most important ones are metal dihalides and transition metal dichalcogenides. Among the low symmetry layer crystals, the most detailed work has been carried out on the orpiment structure [7]. The crystal structures and spectroscopic selection rules have been discussed in the previous sections for all the different types of compounds. In the following we discuss the experimental results obtained on these compounds by different workers. Special features of the observed spectra, particularly those peculiar to the layerlike nature of these compounds, will be pointed out.

A. Metal Halides

In the following we discuss the vibrational spectra of the layered metal halides having CdI_2- and $CdCl_2$-type structures. The experimental data on trihalides and mixed crystals are relatively few and are discussed at the end of this section.

1. CdI_2-Type

Among the layer crystals having a CdI_2-type structure, cadmium and lead iodide crystals were first studied by Mon [36] who assigned a few fundamental and combination bands in the Raman and IR spectra. The IR and Raman measurements of CdI_2 have been repeated by several workers [37–41] with higher precision and higher resolution. Lucovsky and White [39] reported the IR reflectance spectra of CdI_2 and PbI_2 and found large LO-TO splitting in such crystals. Their observations show that LO-TO splitting is larger for the shear (in-plane) modes. The frequencies of the compressional (out-of-plane) modes are found to be larger. They also obtained the optical frequency dielectric constant,

TABLE 8

Intralayer Vibration Frequencies (cm^{-1}) in CdI_2-type Crystals

Crystal	A_{1g}	E_g	A_{2u}	E_u
CdI_2	111.5	43.5[a]	136 (TO)[b] 152 (LO)[b]	79 (TO)[b] 132 (LO)[b]
PbI_2	96[c]	74[c]	96 (TO)[b] 121 (LO)[b]	52 (TO)[b] 108 (LO)[b]
VCl_2[d]	247	198	320 (TO)	275 (TO)
VBr_2[d]	158	120	261 (TO)	225 (TO)
VI_2[d]	115	90	220 (TO)	200 (TO)
$MnBr_2$[e]	151	90	234 (TO) 263 (LO)	143 (TO) 225 (LO)
$FeBr_2$[e]	159	94	231 (TO)	154 (TO)
$CoBr_2$[e]	162	98	230 (TO) 248 (LO)	161 (TO) 212 (LO)
CoI_2[f]			185 (TO) 191 (LO)	152 (TO) 175 (LO)

[a] Ref. 37.

[b] Ref. 39.

[c] Ref. 47.

[d] Ref. 48.

[e] Refs. 49 and 50.

[f] Ref. 51.

oscillator strength, damping, and macroscopic IR effective charges. From a study of 4H-CdI_2, the rigid layer mode frequency has been found at $\omega_L = 15.9$ cm^{-1} [42]. In the case of PbI_2, the earlier discrepancies [43-45] regarding assignments were resolved through the work of Zallen and Slade [46]. The observed intralayer mode frequencies for CdI_2 and PbI_2 structures are collected in Table 8 along with other crystals having the CdI_2-type structure.

The vanadium dihalide crystals VCl_2, VBr_2, and VI_2 have been studied recently in detail by Raman and far-IR spectroscopy [48]. The Raman spectra at low temperature revealed some anomalous features. The additional scattering observed in the case of VCl_2 and VBr_2 has been explained as Raman scattering by spin-phonon coupling via exchange modulation mechanism. Three new lines appeared in the Raman spectra of VI_2 below its Neel temperature; they were attributed to zone-boundary-phonon Raman scattering induced by Bragg scattering from the spin superstructure. The difference in the observed features in VI_2 compared to VCl_2 and VBr_2 is due to their different magnetic properties. These experiments revealed the influence of magnetic order on the vibrational Raman scattering. The collection of the observed zone-center-phonon frequencies of vanadium dihalides given in Table 8 shows that they follow the same pattern of frequency distribution as observed in other CdI_2-type crystals.

Recent Raman scattering measurements [47] on 2H, 4H, 6H, 8H, 12H, and 12R polytypes of PbI_2 at T = 50 and 400 K show that the influence of two-dimensional character on the vibrational spectrum is small, although PbI_2 has a strong layerlike nature. The splitting of vibrational modes in going from lower to higher polytypes is evident from Table 9. A comparison of the spectrum of 2H-PbI_2 with those of higher polytypes reveal the following: (1) appearance of low frequency modes corresponding to the interlayer vibration in multiple cell polytypes and (2) splitting of a few $\underset{\sim}{q} = 0$ modes into multiplets in higher polytypes. It is interesting to note that most of these features have been observed for shear modes (E-type). All the predicted shear (E) interlayer modes have been observed for 4H (E_2), 6H (2E), 8H (3E), and 12H (5E) polytypes (Table 10). The 12R-polytype does not exhibit any such low frequency vibration. The low temperature spectrum at 50 K shows that the shear mode (E_g) at 77.5 cm^{-1} of 2H-polytype splits into a doublet at 74.6 (E_2) and 78.1 (E_1) cm^{-1} in 4H-PbI_2. The same mode splits into a single E line at 77.9 (E^1) and two coinciding lines at 75.5 (E^2, E^3) cm^{-1} in 6H-PbI_2. Four such lines predicted from factor group analysis of 8H-PbI_2 are observed at 77.9 (E^1), 74.3 (E^4), and two coinciding lines at 76.3 (E^2, E^3) cm^{-1}. The 12H polytype shows only two lines at 78.5 and 75.0 cm^{-1} which have been assigned to E^1 and E^2, E^3 (or E^4, E^5). In the case

TABLE 9

Normal Modes in Different Polytypes of PbI_2

Polytypes	2H	4H	6H	8H	12H	12R
Factor group	D_{3d}	C_{6v}	C_{3v}	C_{3v}	C_{3v}	D_{3d}
No. of formula units in a crystal unit cell	1	2	3	4	6	2
Γ_{total}	$A_{1g} + 2A_{2u} + E_g + 2E_u$	$3A_1 + 3B_1 + 3E_1 + 3E_2$	$9A_1 + 9E$	$12A_1 + 12E$	$18A_1 + 18E$	$2A_{1g} + 4A_{2u} + 2E_g + 4E_u$
$\Gamma_{acoustic}$	$A_{2u} + E_u$	$A_1 + E_1$	$A_1 + E$	$A_1 + E$	$A_1 + E$	$A_{2u} + E_u$
Γ_{IR}	$A_{2u} + E_u$	$2A_1 + 2E_1$	$8A_1 + 8E$	$11A_1 + 11E$	$17A_1 + 17E$	$3A_{2u} + 3E_u$
Γ_{Raman}	$A_{1g} + E_g$	$2A_1 + 2E_1 + 3E_2$	$8A_1 + 8E$	$11A_1 + 11E$	$17A_1 + 17E$	$2A_{1g} + 2E_g$

TABLE 10

Interlayer Modes (shear type) and Splitting of E_g Mode at 50 K in Higher Polytypes of PbI_2[a]

Polytype	Frequency (cm^{-1})	Vibrational mode
2H	77.5	E_g
	15.2	E_2^3
4H	74.6	E_2^1
	78.1	E_1^1
6H	13.8	E^8, E^9
	75.5	E^2, E^3
	77.9	E^1
8H	11.8	E^{10}, E^{11}
	15.2	E^{12}
	74.3	E^4
	76.3	E^2, E^3
	77.9	E^1
12H	75.0	E^2, E^3 or E^4, E^5
	78.0	E^1
12R	74.6	E_g^2
	78.1	E_g^1

[a]Ref. 47.

of 12H-polytype it is difficult to discern the spectrum because the observed scattering is small; in fact, this gets steadily smaller the higher the polytype. All these observed data are used by Sears, Klein, and Morrison [47] in a fit of force constant parameters using a

simple force constant model [52, 53] to be discussed later. The calculated force constants for intra- and interlayer motions lead to the conclusion that PbI_2 has a less layerlike nature than MoS_2. The large amount of information obtained for interlayer vibration frequencies and Davydov splittings in higher polytype may be used in more refined calculation of interlayer force, mode coupling, and the consequent effect on the dynamics of polytypes.

A very important feature of the CdI_2-type layer crystals is the large LO-TO splitting. This is a manifestation of large anisotropy and the existence of long-range dipole-dipole interaction. Detailed theoretical discussions of LO-TO splitting are given in standard texts [15, 54].

2. $CdCl_2$-Type

Among the $CdCl_2$-type layer crystals, the vibrational spectra have been reported for chlorides of Mg, Mn, Fe, Co, Ni, and Cd; bromides of Ni and Cd; and the iodide of Ni. The transition metal dihalides are useful hosts for studying iron group transition metal ions. ESR [55], Jahn-Teller effect [56], and many other optical [57] experiments have been carried out on doped $CdCl_2$-type lattices. A knowledge of lattice vibrations of these crystals is a prerequisite for interpretation of these observed data. This has induced a number of useful studies on the vibrational spectra of $CdCl_2$-type crystals.

The first detailed study of the optical mode frequencies of $CdCl_2$, $CdBr_2$, $MnCl_2$, and $CoCl_2$ was that of Lockwood [58]. The Raman and IR studies were recorded on powder specimens dispersed in polyethylene. His assignment of IR active E_u modes was not correct. This was pointed out by Campbell [59] from a study of thin layers of $CdBr_2$ produced by stripping with a sellotape. The thinnest sample produced by this technique was 2.5 μm thick. His [59] measurements show that the E_u (TO) mode frequency is much lower than that of Lockwood [58]. This is also confirmed by the IR observation of Marioka and Nakagawa [40] for both $CdCl_2$ and $CdBr_2$. More recent investigations [49, 50] present a comprehensive picture of the vibrational spectra of these crystals. These data are presented in Table 11 together with those by Nakashima et al. [37] and Marioka and Nakagawa [40]. These crystals also exhibit a large amount of LO-TO splitting for IR-active modes.

Besides the vibrational spectroscopic experiments aimed purely at solving the dynamical problem, a large number of spectroscopic experiments based on the unusual magnetic properties and strong magnon-phonon interactions have recently been reported for transition metal dihalides. In addition to determining the Raman-active phonons, these studies yielded information about the ground state of metal ion by electronic Raman scattering and magnons. The studies were carried out mostly by Lockwood and co-workers [60-64].

TABLE 11

Intralayer Vibration Frequencies (cm^{-1}) of $CdCl_2$-type Crystals

Crystal	A_{1g}	E_g	A_{2u}	E_u
$CdCl_2$	233.5[a]	133.5[a]	137.2 (TO)[b] 223.6 (LO)[b]	152 (TO)[c] 233 (LO)[c]
$CdBr_2$	146[a]	74.5[a]	99.1 (TO)[b] 164.0 (LO)[b]	104 (TO)[c] 178 (LO)[c]
$MnCl_2$[d]	235	144	255 (TO) 308 (LO)	185 (TO) 276 (LO)
$FeCl_2$[d]	250	150	270 (TO) 315 (LO)	192 (TO) 271 (LO)
$CoCl_2$[d]	253	156	277 (TO) 317 (LO)	206 (TO) 272 (LO)
$NiCl_2$[d]	269	173	293 (TO) 324 (LO)	225 (TO) 270 (LO)
$NiBr_2$[d]	168	106	230 (TO) 248 (LO)	181 (TO) 212 (LO)
NiI_2[e]			178 (TO) 184 (LO)	156 (TO) 176 (LO)

[a] Ref. 37.

[b] Calculated values in Ref. 40.

[c] Ref. 40.

[d] Refs. 49 and 50.

[e] Ref. 51.

3. Trihalides and Mixed Halides

Among the trihalide layer crystals only $FeCl_3$ has been studied by Raman spectroscopy. The crystal has BiI_3-type structure [65]. The IR and Raman spectra of PbFX (X = Cl, Br, I) have been reported by

Rulmont [66] on powder samples. The assignments were made from a study of oriented flaky crystals. Raman polarization data were also obtained on a single crystal of PbFCl.

Caswell and Solin [65] studied the polarized Raman spectra of $FeCl_3$ and Stage 1 and 2 graphite-$FeCl_3$ intercalation compounds. The crystal space group is C_{3i}^2 ($R\bar{3}$). The layer factor group is D_{3d}. For both the crystal and the layer the primitive unit cell contains two $FeCl_3$ molecular units. Thus the total number of optically active modes is 24 for both the crystal and layer factor groups. However, the symmetry species attached would be different. We have

$$\Gamma^{\text{crystal}} = 4A_g + 3A_u + 4E_g + 3E_u$$

and

$$\Gamma^{\text{layer}} = 2A_{1g} + 2A_{2g} + A_{1u} + 2A_{2u} + 4E_g + 3E_u$$

for the optical modes. The correlation is straightforward. The observed Raman frequencies show that $FeCl_3$ intercalated with graphite maintains the layer structure. There was no evidence of monomeric $FeCl_3$ or dimeric Fe_2Cl_6, nor for $FeCl_2$ layer stoichiometry.

B. Metal Hydroxides

Among the metal hydroxides $Mg(OH)_2$ has been of interest to spectroscopists since 1905 [1]. Since then the large number of papers [2-5] published have been reviewed by Mitra [6]. The assignment of vibrational modes have been changed many times [67], and the latest work by Dawson, Hadfield, and Wilkinson [68] on $Mg(OH)_2$ and $Ca(OH)_2$ provides the correct assignment of symmetry modes. These metal hydroxide crystals occupy a special position in the group of layer crystals. They contain molecular groups OH and exhibit factor group splitting of OH intramolecular vibrational mode. However, there is no Davydov splitting since the unit cell contains only one layer. It may be noted that the OH internal mode splitting has been defined as Davydov splitting in earlier works. These crystals possess features common to both layer and molecular crystals. The vibrational modes in these cases may be classified as internal and external; external modes can be divided into two types—translational and rotational (or librational). Factor group analysis of normal modes with D_{3d} symmetry yield